

Multi-Task Convolutional Neural Network for Face Recognition

Xi Yin, Xiaoming Liu

Department of Computer Science and Engineering
Michigan State University, East Lansing MI 48824

{yinxil, liuxm}@msu.edu

Abstract

This paper explores multi-task learning (MTL) for face recognition. We answer the questions of how and why MTL can improve the face recognition performance. First, we propose a multi-task Convolutional Neural Network (CNN) for face recognition where identity recognition is the main task and pose, illumination, and expression estimations are the side tasks. Second, we develop a dynamic-weighting scheme to automatically assign the loss weight to each side task. Third, we propose a pose-directed multi-task CNN by grouping different poses to learn pose-specific identity features, simultaneously across all poses. We observe that the side tasks serve as regularizations to disentangle the variations from the learnt identity features. Extensive experiments on the entire Multi-PIE dataset demonstrate the effectiveness of the proposed approach. To the best of our knowledge, this is the first work using all data in Multi-PIE for face recognition. Our approach is also applicable to in-the-wild datasets for pose-invariant face recognition and we achieve comparable or better performance than state of the art on LFW, CFP, and IJB-A.

1. Introduction

Face recognition is a challenging problem due to its variations in Pose, Illumination, Expression (PIE), and etc. Recent CNN-based approaches mainly focus on exploring the effects of 3D model-based face alignment [32], larger datasets [32, 28], or new loss functions [30, 28, 22, 35]. Most existing methods consider face recognition as a single task of extracting robust identity features. We believe that face recognition is not an isolated problem — often tangled with other tasks. For example, when a human being is presented a face image, he will instinctively recognize the identity and expression at the same time. This motivates us to explore multi-task learning for face recognition.

Multi-task learning (MTL) aims to learn several tasks simultaneously to boost the performance of the main task or all tasks. It has been successfully applied to face detec-

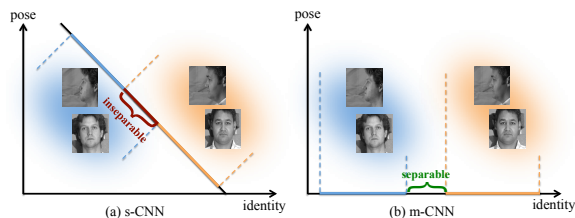


Figure 1. We propose MTL to disentangle the PIE variations from learnt identity features. (a) For single-task learning, the main variance is captured in x - y , resulting in an inseparable region between these two subjects. (b) For multi-task learning, identity is separable in x -axis by excluding y -axis that models pose variation.

tion [4, 40], face alignment [42], pedestrian detection [33], attribute estimation [1], and so on. Despite the success of MTL in various vision problems, there is a lack of comprehensive study of MTL for face recognition. In this paper, we study face recognition as a multi-task problem where identity classification is the main task with PIE estimations being the side tasks. We answer the questions of how and why PIE estimations can help face recognition.

We incorporate MTL into the CNN framework for face recognition. We assume that different tasks share the same feature representation, which is learnt through several convolution and pooling layers. A fully connected layer is added to the shared features for the classification of each task. The side tasks serve as regularizations to learn more discriminative identity features. As shown in Fig. 1, when identity (x axis) is mixed with pose variation (y axis), single-task learning (s-CNN) for face recognition may learn a joint decision boundary along x - y , resulting in an inseparable region between different identities. In contrary, with multi-task learning (m-CNN), the shared feature space is learnt to model identity and pose separately. The identity features can exclude pose variation by selecting only the key dimensions that are essential for face recognition.

One problem with MTL is how to weight the importance of different tasks. Prior work either treat different tasks equally [39] or obtain the weights by greedy search [33]. We believe that our side tasks contribute differently to face recognition. However, it will be very time consuming or

setting	session	pose	exp	illum	train subjects / images	gallery / probe images	total	references
I	4	7	1	1	200 / 5,383	137 / 2,600	8,120	[3, 20]
II	1	7	1	20	100 / 14,000	149 / 20,711	34,860	[44, 39]
III	1	15	1	20	150 / 45,000	99 / 29,601	74,700	[36]
IV	4	9	1	20	200 / 138,420	137 / 70,243	208,800	[45, 39]
ours	4	15	6	20*	200 / 498,900	137 / 255,163	754,200	

Table 1. Comparison of the experimental settings that are commonly used in prior work on the Multi-PIE dataset. (* The 20 images consist of 2 duplicates of non-flash images and 18 flash images. In total there are 19 different illuminations.)

practically impossible to find the optimal weights for all side tasks via brute-force search. We propose to use dynamic weights where we only determine the overall importance for PIE estimations, and the CNN can learn to dynamically assign a loss weight to each side task during training. This is effective and efficient as will be shown in Sec. 4.

Since pose variation is the most challenging one among non-identity variations, and the proposed m-CNN already classifies all training images into different pose groups, we propose to apply divide-and-conquer to CNN learning. Specifically, we develop a novel pose-directed multi-task CNN (p-CNN) where the pose estimation can categorize the training data into three different pose groups, direct them through different routes in the network to learn pose-specific identity features in addition to the generic identity features. Similarly, the loss weights for extracting these two types of features are determined dynamically in the CNN framework. We find this technique to be effective in handling pose variation in face recognition.

This work utilizes *all* data in Multi-PIE [10], i.e., faces with the full range of PIE variations, as the main experimental dataset – ideal for studying MTL for face recognition. To the best of our knowledge, there is no prior face recognition work that studies the full range of variations in Multi-PIE. Further, we apply our method to in-the-wild datasets where the ground truth label of the side task is unavailable.

We make four contributions: (1) we explore how and why PIE estimations can help face recognition; (2) we propose a dynamic-weighting scheme to learn the loss weights for different tasks automatically in the CNN framework; (3) we develop a pose-directed multi-task CNN to handle pose variation; (4) this is the most comprehensive and first face recognition study on entire Multi-PIE. We achieve comparable or superior performance to state-of-the-art methods on Multi-PIE, LFW [13], CFP [29], and IJB-A [19].

2. Prior Work

Face Recognition We focus our review on face recognition methods related to handling pose variation and MTL. Most existing work of single-task face recognition treat each pose separately by learning different models for different poses. For example, Masi et al. [23] propose pose-aware face recognition by learning a specific model for each type of face alignment and pose group. Xiong et al. [36] pro-

pose a conditional CNN for face recognition, which can discover the modality information automatically during training. The idea of divide-and-conquer is similar to our work. Differently, we utilize the side task labels to learn variation disentangled identity features. Ding et al. [8] propose to transform the features of different poses into a discriminative subspace, and the transformations are learnt jointly for all poses with one task for each pose. [39] develops a deep neural network to rotate a face image while preserving the identity, and the reconstruction of the face is considered as a side task. In this work, we treat face recognition as a multi-task problem with PIE estimations as the side tasks to disentangle PIE variations from the identity features. Our proposed p-CNN can jointly learn generic and pose-specific identity features in one framework.

Multi-Task Learning It is commonly assumed in MTL that different tasks share the same features. Traditional linear model parameterizes each task with a weight vector. The weight vectors of all tasks form a weight matrix, which is regularized by $l_{2,1}$ norm [2] or trace norm [15] to encourage a low-rank matrix. It is natural to fuse MTL with CNN to learn the shared features and the task-specific models. For examples, Misra et. al. [24] propose a cross-stitch network for MTL to learn the sharing strategy, which is difficult to scale to multiple tasks. In [40], a task-constrained deep network is developed for landmark detection with facial attribute classifications as the side tasks. However, the roles of the auxiliary tasks are not clear. In this work, we discover that the side tasks of PIE estimations serve as regularizations to learn more discriminative identity features that are robust to PIE variations.

In MTL, it is important to determine the loss weights for different tasks. The work of [39] uses equal weights for the tasks of face recognition and face frontalization. Tian et al. [33] propose to fix the weight for the main task as 1, and obtain the weights of all side tasks via greedy search within 0 and 1. Let n and k be the number of side tasks and searched values respectively. This approach has two drawbacks. First, it is very inefficient as the computation scales to the number of tasks (complexity nk). Second, the optimal weight obtained for each task may not be jointly optimal. Further, the complexity would be k^n if we search all combinations in a brute-force way. In contrast, we propose

a dynamic-weighting mechanism where we only determine the overall weight for all side tasks (complexity k) and let CNN learn to distribute the weights for each side task.

Multi-PIE Multi-PIE dataset consists of 754,200 images of 337 subjects with PIE variations. As a classic face dataset, it has been used to study face recognition robust to pose [20, 18], illumination [12, 11], and expression [7, 43]. Most prior work study the combined variations of pose and illumination [8, 41, 45] with increasing pose variation from half-profile [41] to a full range [36]. Chu et al. [7] propose a framework for pose normalization and expression neutralization by using an extended 3D Morphable Model. The work of [37] develops a sparse variation dictionary learning to study face recognition under a subset of PIE variations. However, only a very small subset is selected for experiments in [7, 37]. To the best of our knowledge, this is the first effort using the entire set of Multi-PIE to study face recognition under a full span of PIE variations. A comparison of different experimental settings is shown in Tab. 1.

3. The Proposed Approach

In this section, we demonstrate our methods on Multi-PIE dataset and extend it to unconstrained datasets in the experiments. First, we propose a multi-task CNN (m-CNN) with dynamic weights for face recognition (the main task) and PIE estimations (the side tasks). Second, we propose a pose-directed multi-task CNN (p-CNN) to tackle pose variation by separating all poses into different groups and jointly learning identity features for each group.

3.1. Multi-Task CNN

Any CNN-based face recognition needs a good network to build upon. In our case, we adapt CASIA-Net [38], which has proved to work well on LFW dataset, with three modifications. First, batch normalization (BN) [14] is applied to accelerate the training process. Second, the contrastive loss is excluded to simplify our loss function. Third, the dimension of the fully connected layer is changed according to different tasks. Details of the layer parameters are shown in Fig. 2. The network consists of five blocks each including two convolution layers and a pooling layer. BN and ReLU [25] are used after each convolution layer, which are omitted for clarity. Similar to [38], no ReLU is used after conv52 to learn a compact feature representation, and a dropout layer with a ratio of 0.4 is applied after pool5.

Given a set of N training images and their labels: $\mathbf{D} = \{\mathbf{I}_i, \mathbf{y}_i\}_{i=1}^N$, where each label \mathbf{y}_i is a vector consisting of the identity label y_i^d and the side task labels. In this paper, we consider three side tasks including pose (y_i^p), illumination (y_i^l), and expression (y_i^e). We eliminate the sample index i for clarity. As shown in Fig. 2, the proposed m-CNN ex-

tracts a high-level feature representation $\mathbf{x} \in \mathbb{R}^{D \times 1}$:

$$\mathbf{x} = f(\mathbf{I}; \mathbf{k}, \mathbf{b}, \gamma, \beta), \quad (1)$$

where $f(\cdot)$ represents the non-linear mapping from the input image to the shared features. \mathbf{k} and \mathbf{b} are the sets of filters and bias of all convolutional layers. γ and β are the sets of scales and shifts in all BN layers. Let $\Theta = \{\mathbf{k}, \mathbf{b}, \gamma, \beta\}$ denote all parameters to be learnt to extract the features.

The extracted features \mathbf{x} , which is pool5 in our model, are shared among all tasks. Suppose $\mathbf{W}^d \in \mathbb{R}^{D \times D_d}$ and $\mathbf{b}^d \in \mathbb{R}^{D_d \times 1}$ are the weight matrix and bias vector in the fully connected layer for identity classification, where D_d is the number of different identities in \mathbf{D} . The generalized linear model can be applied:

$$\mathbf{y}^d = \mathbf{W}^{d\top} \mathbf{x} + \mathbf{b}^d. \quad (2)$$

\mathbf{y}^d is fed to a softmax layer to compute the probability of \mathbf{x} belonging to each subject in the training set.

$$\text{softmax}(\mathbf{y}^d)_n = p(\hat{y}^d = n | \mathbf{x}) = \frac{\exp(\mathbf{y}_n^d)}{\sum_j \exp(\mathbf{y}_j^d)}, \quad (3)$$

where \mathbf{y}_j^d is the j th element in \mathbf{y}^d . The $\text{softmax}(\cdot)$ function converts the model output \mathbf{y}^d to a probability distribution over all subjects and the subscript selects the n th element. Finally, the estimated identity \hat{y}^d is obtained via:

$$\hat{y}^d = \underset{n}{\operatorname{argmax}} \quad \text{softmax}(\mathbf{y}^d)_n. \quad (4)$$

Then the cross-entropy loss can be employed:

$$L(\mathbf{I}, \mathbf{y}^d) = -\log(p(\hat{y}^d = y^d | \mathbf{I}, \Theta, \mathbf{W}^d, \mathbf{b}^d)). \quad (5)$$

Similarly, we formulate the losses of the side tasks. Let $\mathbf{W} = \{\mathbf{W}^d, \mathbf{W}^p, \mathbf{W}^l, \mathbf{W}^e\}$ represent the weight matrices for identity and PIE classifications. The bias terms are eliminated for simplicity. Given the training set \mathbf{D} , our m-CNN aims to minimize the combined loss of all tasks:

$$\underset{\Theta, \mathbf{W}}{\operatorname{argmin}} \quad \alpha_d \sum_{i=1}^N L(\mathbf{I}_i, y_i^d) + \alpha_p \sum_{i=1}^N L(\mathbf{I}_i, y_i^p) + \alpha_l \sum_{i=1}^N L(\mathbf{I}_i, y_i^l) + \alpha_e \sum_{i=1}^N L(\mathbf{I}_i, y_i^e), \quad (6)$$

where $\alpha_d, \alpha_p, \alpha_l, \alpha_e$ control the importance of each task. It becomes a single-task model (s-CNN) when $\alpha_{p,l,e} = 0$. The loss drives the model to learn both the parameters Θ for extracting the shared features and \mathbf{W} for the classification tasks. In the testing stage, the features before the softmax layer (\mathbf{y}^d) are used for face recognition by applying a face matching procedure based on cosine similarity.

3.2. Dynamic-Weighting Scheme

In CNN-based MTL, it is an open question on how to set the loss weight for each task. Prior work either treat

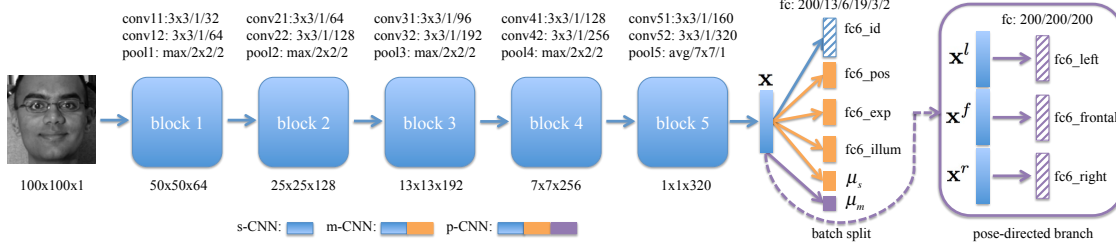


Figure 2. The proposed m-CNN and p-CNN for face recognition. Each block reduces the spatial dimensions and increases the channels of the feature maps. The formats for the convolution and pooling parameters are: filter size / stride / filter number and method / filter size / stride. The feature dimensions after each block operation are shown on the bottom. The dashed line represents the batch split operation as shown in Fig. 3. The layers with the stripe pattern are the identity features used in the testing stage for face recognition.

all tasks equally [39] or obtain weights via brute-force search [33]. However, it is very time-consuming to search for all weight combinations. To solve this problem, we propose a dynamic-weighting scheme to automatically assign loss weights to each side task during training.

First, the weight for the main task is set to 1, i.e. $\alpha_d = 1$. Second, instead of finding the loss weight for each task, we find the summed loss weight for all side tasks, i.e. $\varphi_s = \alpha_p + \alpha_l + \alpha_e$, via brute-force search in a validation set. Our m-CNN learns to allocate φ_s to three side tasks. As shown in Fig. 2, we add a fully connected layer and a softmax layer to the shared features \mathbf{x} to learn the dynamic weights. Let $\omega_s \in \mathbb{R}^{D \times 3}$ and $\epsilon_s \in \mathbb{R}^{3 \times 1}$ denote the weight matrix and bias vector in the fully connected layer,

$$\mu_s = \text{softmax}(\omega_s^T \mathbf{x} + \epsilon_s), \quad (7)$$

where $\mu_s = [\mu_p, \mu_l, \mu_e]^T$ are the dynamic loss weights for the side tasks with $\mu_p + \mu_l + \mu_e = 1$. So Eqn. 6 becomes:

$$\begin{aligned} \argmin_{\Theta, \mathbf{W}, \omega_s} \quad & \sum_{i=1}^N L(\mathbf{I}_i, y_i^d) + \varphi_s \left[\mu_p \sum_{i=1}^N L(\mathbf{I}_i, y_i^p) + \right. \\ & \left. \mu_l \sum_{i=1}^N L(\mathbf{I}_i, y_i^l) + \mu_e \sum_{i=1}^N L(\mathbf{I}_i, y_i^e) \right] \\ \text{s.t.} \quad & \mu_p + \mu_l + \mu_e = 1. \end{aligned} \quad (8)$$

We use mini-batch stochastic gradient descent to solve the above optimization problem where the dynamic weights are averaged over a batch of samples. Intuitively, we expect our m-CNN to behave in two different aspects in order to minimize the loss. First, since our main task contribute mostly to the final loss ($\varphi_s < 1$), the side task with the largest contribution to the main task should have the highest weight in order to reduce the loss of the main task. Second, our m-CNN should assign a higher weight for an easier task with a lower loss so as to reduce the overall loss. We have observed these effects as shown in Fig. 5 (a).

3.3. Pose-Directed Multi-Task CNN

It is very challenging to learn a non-linear mapping to estimate the correct identity from a face image with arbitrary

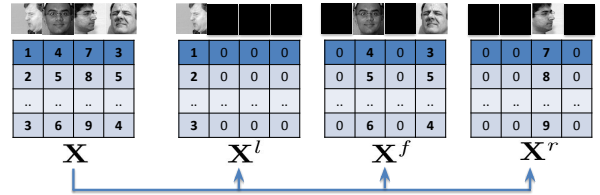


Figure 3. Illustration of the batch split operation in p-CNN.

PIE, given the diverse variations in the data. This challenge has been encountered in classic pattern recognition work. For example, in order to handle pose variation, [21] proposes to construct several face detectors where each of them is in charge of one specific view. Such a divide-and-conquer scheme can be applied to CNN learning because the side tasks can “divide” the data and allow the CNN to better “conquer” them by learning tailored mapping functions. Therefore, we propose a novel task-directed multi-task CNN where the side task categorizes the training data into multiple groups, and directs them to different routes in the network. Since pose is considered as the primary challenge in face recognition [36, 41, 45], we propose pose-directed multi-task CNN (p-CNN) to handle pose variation. However, it is applicable to any other variation.

As shown in Fig. 2, p-CNN is built on top of m-CNN by adding the pose-directed branch (PDB). The PDB groups face images with similar poses to learn pose-specific identity features via a batch split operation. We separate poses into three groups: left profile (G^l), frontal (G^f), and right profile (G^r). As shown in Fig. 3, the goal of batch split is to separate a batch of N_0 samples ($\mathbf{X} = \{\mathbf{x}_i\}_{i=1}^{N_0}$) into three batches \mathbf{X}^l , \mathbf{X}^f , and \mathbf{X}^r , which are of the same size as \mathbf{X} . During training, the ground truth pose is used to assign a face image into the correct group. Let us take the frontal group as an example:

$$\mathbf{x}_i^f = \begin{cases} \mathbf{x}_i, & \text{if } y_i^p \in G^f \\ \mathbf{0}, & \text{otherwise,} \end{cases} \quad (9)$$

where $\mathbf{0}$ denotes a vector of all zeros with the same dimension as \mathbf{x}_i . The assignment of $\mathbf{0}$ is to avoid the case when no sample is passed into one group, the next layer may

still have valid input. Therefore, \mathbf{x}^n is separated into three batches where each batch consists of only the samples belonging to the corresponding pose group. Each group learns a pose-specific mapping to a joint space, resulting in three different sets of weights: $\{\mathbf{W}^l, \mathbf{W}^f, \mathbf{W}^r\}$. Finally the features from all groups are merged as the input to a softmax layer to perform robust identity classification jointly.

Our p-CNN aims to learn two types of identity features: \mathbf{W}^d is the weights to extract generic identity features that is robust to all poses; $\mathbf{W}^{l,f,r}$ are the weights to extract pose-specific identity features that are robust within a small pose range. Both tasks are considered as our main tasks. Similar to the dynamic-weighting scheme in m-CNN, we use dynamic weights to combine our main tasks as well. The summed loss weight for these two tasks is $\varphi_m = \alpha_d + \alpha_g$. Let $\omega_m \in \mathbb{R}^{D \times 2}$ and $\epsilon_m \in \mathbb{R}^{2 \times 1}$ denote the weight matrix and bias vector for learning the dynamic weights,

$$\mu_m = \text{softmax}(\omega_m^\top \mathbf{x} + \epsilon_m). \quad (10)$$

We have $\mu_m = [\mu_d, \mu_g]^\top$ as the dynamic weights for generic identity classification and pose-specific identity classification. Finally, the loss of p-CNN is formulated as:

$$\begin{aligned} \underset{\Theta, \mathbf{W}, \omega}{\text{argmin}} \quad & \varphi_m \left[\mu_d \sum_{i=1}^N L(\mathbf{I}_i, y_i^d) + \mu_g \sum_{g=1}^G \sum_{i=1}^{N_g} L(\mathbf{I}_i, y_i^g) \right] + \\ & \varphi_s \left[\mu_p \sum_{i=1}^N L(\mathbf{I}_i, y_i^p) + \mu_l \sum_{i=1}^N L(\mathbf{I}_i, y_i^l) + \mu_e \sum_{i=1}^N L(\mathbf{I}_i, y_i^e) \right] \quad (11) \\ \text{s.t.} \quad & \mu_d + \mu_g = 1, \quad \mu_p + \mu_l + \mu_e = 1, \end{aligned}$$

where G is the number of pose groups, and N_g is the number of training images in the g -th group. $\omega = \{\omega_m, \omega_s\}$ is the set of parameters to learn the dynamic weights for both the main and side tasks. We set $\varphi_m = 1$.

Stochastic Routing During testing, we can use the estimated pose to direct an image to extract pose-specific features. However, the pose estimation error may cause inferior feature extraction, especially for unconstrained faces. To solve this problem, we propose a stochastic routing scheme. Specifically, given a test image \mathbf{I} , we extract the generic features (\mathbf{y}^d) and pose-specific features ($\{\mathbf{y}^g\}_{g=1}^G$) by directing it to all paths in the PDB. We can also obtain the probabilities of image \mathbf{I} belonging to each pose group as ($\{p^g\}_{g=1}^G$) using our pose estimation side task. The distance between a pair of face images (\mathbf{I}_1 and \mathbf{I}_2) is computed as:

$$s = \frac{1}{2} d(\mathbf{y}_1^d, \mathbf{y}_2^d) + \frac{1}{2} \sum_{i=1}^G \sum_{j=1}^G d(\mathbf{y}_1^i, \mathbf{y}_2^j) \cdot p_1^i \cdot p_2^j, \quad (12)$$

where $d(\cdot)$ is a distance metric used to compute the feature distance. The proposed stochastic routing accounts for all combinations of pose-specific features weighted by the probabilities. This is more robust to pose estimation errors. We treat the generic features and pose-specific features equally and fuse them for face recognition.

4. Experiments

We evaluate the proposed method under two settings: (1) face identification on Multi-PIE; (2) face verification/identification on in-the-wild datasets: LFW, CFP, and IJB-A. We use Caffe [16] with our modifications.

4.1. Face Identification on Multi-PIE

Experimental settings Multi-PIE dataset consists of 754,200 images of 337 subjects recorded in 4 sessions. Each subject was recorded with 15 different cameras where 13 at the head height spaced at 15° interval and 2 above the head to simulate a surveillance camera view, labeled as $\pm 45^\circ$ in our work. For each camera, a subject was imaged under 19 different illuminations. In each session, a subject was captured with 2 or 3 expressions, resulting in 6 different expressions across all sessions. In our work, we use the entire dataset. The first 200 subjects are used for training. The remaining 137 subjects are used for testing, where one image with frontal pose, neutral illumination and neutral expression for each subject is selected as the gallery set and the remaining as the probe set.

We use the landmark annotations [9] to align each face to a canonical view of size 100×100 . We normalize the image by subtracting 127.5 and dividing by 128, similar to [35]. The momentum is set to 0.9 and the weight decay to 0.0005. All models are trained for 20 epochs from scratch with a batch size of 4. The learning rate starts at 0.01 and reduces at 10th, 15th, and 19th epochs with a factor of 0.1. The features before the softmax layer are used for face matching based on cosine similarity. The rank-1 identification rate is reported as the face recognition performance. For the side tasks, the mean accuracy over all classes is reported.

Effects of MTL To evaluate the influence of MTL, we train four single-task models (s-CNN) for identity (id), pose (pos), illumination (illum), and expression (exp) classification, respectively. For MTL, we split 10% training subjects for validation and obtain the optimal value of $\varphi_s = 0.1$ via brute-force search. In order to evaluate the influence of each side task, we add only one side task to the main task and set its loss weight to 0.1. We use “id+pos”, “id+illum”, and “id+exp” to represent these variants and compare them to the performance of adding all side tasks denoted as “id+all”. Furthermore, to evaluate the effects of dynamic-weighting scheme, we train a model with fixed loss weights for the side tasks as: $\alpha_p = \alpha_l = \alpha_e = \varphi_s/3 = 0.033$.

The first row in Tab. 2 shows the performance of single-task learning. The rank-1 identification rate of s-CNN is 75.67% without adding any side task. The performance of the frontal pose group is much higher than that of the profile pose groups, indicating that pose variation is indeed a big challenge for face recognition. Among all side tasks, pose estimation is easiest, followed by illumination, and expression is the most difficult task. This is caused by two poten-

model	loss weights	rank-1 (all / left / frontal /right)	pose	illum	exp
s-CNN	$\alpha_d/\alpha_p/\alpha_l/\alpha_e = 1$	75.67 / 71.51 / 82.21 / 73.29	99.87	96.43	92.44
m-CNN: id+pos	$\alpha_d = 1, \alpha_p = 0.1$	78.06 / 75.06 / 82.91 / 76.21	99.78	—	—
m-CNN: id+illum	$\alpha_d = 1, \alpha_l = 0.1$	77.30 / 74.87 / 82.83 / 74.21	—	93.57	—
m-CNN: id+exp	$\alpha_d = 1, \alpha_e = 0.1$	77.76 / 75.48 / 82.32 / 75.48	—	—	90.93
m-CNN: id+all	$\alpha_d = 1, \alpha_{p,l,e} = 0.033$	77.59 / 74.75 / 82.99 / 75.04	99.75	88.46	79.97
m-CNN: id+all (dynamic)	$\alpha_d = 1, \varphi_s = 0.1$	79.35 / 76.60 / 84.65 / 76.82	99.81	93.40	91.47
m-CNN: id+all (D=640)	$\alpha_d = 1, \varphi_s = 0.1$	78.26 / 75.62 / 83.28 / 75.88	99.83	93.69	91.55
p-CNN	$\varphi_m = 1, \varphi_s = 0.1$	79.55 / 76.14 / 84.87 / 77.65	99.80	90.58	90.02

Table 2. Performance comparison (%) of single-task learning (s-CNN), multi-task learning (m-CNN) with its variants, and pose-directed multi-task learning (p-CNN) on Multi-PIE dataset.

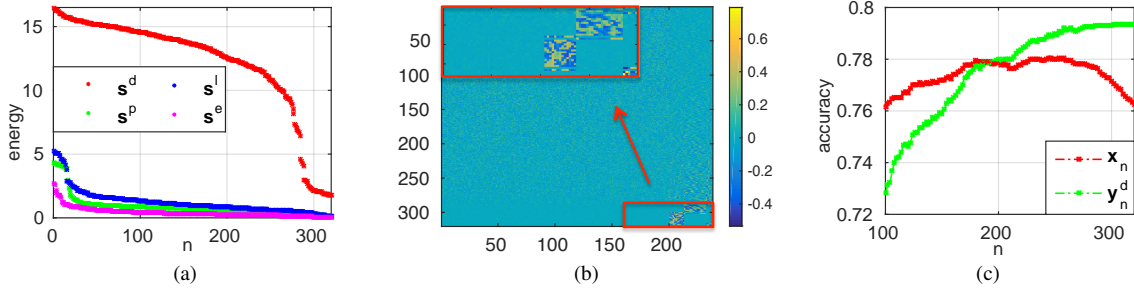


Figure 4. Analysis on the effects of MTL: (a) the sorted energy vectors for all tasks; (b) visualization of the weight matrix \mathbf{W}^{all} where the red box in the top-left is a zoom-in view of the bottom-right; (c) the face recognition performance with varying feature dimensions.

tial reasons. First, discriminating expression is more challenging due to the non-rigid face deformation. Second, the data distribution over different expressions is unbalanced with insufficient training data for some expressions.

Comparing rank-1 identification rates of s-CNN and m-CNNs, it is obvious that adding the side tasks is always helpful for the main task, despite the fact that the side task performance might be similar or slightly worse. The summation of the loss weights for all side tasks are equal to φ_s for all m-CNN variants in Tab. 2 for a fair comparison. The improvement of face recognition is mostly on profile faces with MTL, indicating again that pose is the key variation especially when mixed with other variations. The m-CNN “id+all” with dynamic weights shows superior performance to others not only in rank-1 identification rate, but also in the side task estimations. Further, the lower rank-1 identification rate of “id+all” w.r.t “id+pos” indicates that more side tasks do not necessarily lead to better performance without properly setting the loss weights. In contrast, the proposed dynamic-weighting scheme effectively improves the performance to 79.35% from the fixed weighting of 77.59%.

Why MTL helps? We investigate why PIE estimations are helpful for face recognition. Since all tasks are learnt from the shared representation $\mathbf{x} \in \mathbb{R}^{320 \times 1}$, we analyze the importance of each dimension in \mathbf{x} to each task. We make the assumption that if a feature dimension is important, the corresponding row in the learnt weight matrix should have high absolute values. Take the main task as an example. We compute an energy vector $\mathbf{s}^d \in \mathbb{R}^{320 \times 1}$ whose element is

computed as $s_i^d = \sum_{j=1}^{200} |\mathbf{W}_{ij}^d|$. A higher value in s^d indicates a dimension is more important to face recognition. Similarly, we compute the energy vectors for all side tasks as $\mathbf{s}^p, \mathbf{s}^l, \mathbf{s}^e$ from their weight matrices. We sort each energy vector in a descending order and plot them as shown in Fig. 4 (a). The large variance of each energy vector indicates that each dimension contributes differently to a particular task. Note that the index of the feature dimension is not consistent among them. To compare how each dimension contributes to different tasks, we concatenate the weight matrix of all tasks as $\mathbf{W}_{320 \times 238}^{all} = [\mathbf{W}^d, \mathbf{W}^p, \mathbf{W}^l, \mathbf{W}^e]$ and compute its energy vector as \mathbf{s}^{all} . We sort the rows in \mathbf{W}^{all} based on the descending order in energy, as visualized in Fig. 4 (b). We observe that the shared representation are learnt to allocate a separate set of dimensions for each task, as shown in the block-wise effect in the zoom-in view.

To further validate this observation, we contrast two types of features for face recognition: 1) a subset of \mathbf{x} with the n largest energy in \mathbf{s}^d , which are more crucial in modeling identity variation, 2) the features $\mathbf{y}_{n \times 1}^d = \mathbf{W}_{n \times 200}^d \mathbf{x}_{n \times 1} + \mathbf{b}^d$. We vary n from 100 to 320 and plot the performance in Fig. 4 (c). When \mathbf{x}_n is used, the performance improves with increasing dimensions and drops when additional dimensions are included, which are learnt to model the PIE variations. In contrary, the learnt identity features \mathbf{y}_n^d can eliminate the effects of the dimensions that are not helpful for identity classification through the weight matrix \mathbf{W}^d , resulting in continuously improved performance w.r.t. n . Therefore, we conclude that the side tasks

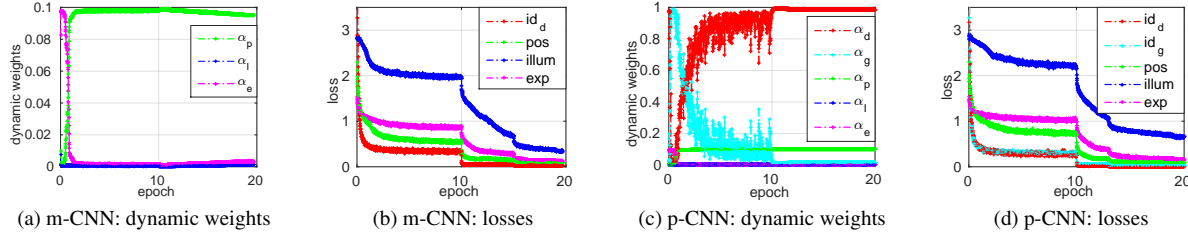


Figure 5. Dynamic weights and losses for m-CNN and p-CNN during the training process.

can disentangle the PIE variations from the shared representation for PIE-invariant face recognition.

Performance of p-CNN For p-CNN, we split all yaw angles into three groups: right profile (-90° , -75° , -60° , -45°), frontal (-30° , -15° , 0° , 15° , 30°), and left profile (45° , 60° , 75° , 90°). Since all tasks are learnt from the shared features \mathbf{x} , it will be too competitive if the dimension is low. So we double the number of filters in the conv52 layer in order to increase the dimension of \mathbf{x} from 320 to 640. The face recognition performance is further improved to 79.55%. For comparison, we train another m-CNN with $D = 640$. As shown in Tab. 2, an increased dimension in \mathbf{x} does not lead to better performance for m-CNN. It is an open question on how many dimensions are needed for different models. We leave it to our future work.

Dynamic-weighting scheme Figure 5 shows the dynamic weights and losses during training. For m-CNN, expression classification has the largest weight in the first epoch as it has the highest chance to be correct with random guess. As training goes on, pose classification takes over because it is the easiest task (highest accuracy in s-CNN) and also most helpful for face recognition (compare id+pos to id+exp and id+illum). α_p starts to decrease at 11th epoch when pose classification is saturated. The increased α_l and α_e cause the reduction in the losses of expression and illumination classifications. As we expected, the dynamic-weighting scheme assigns a higher loss weight for the easiest and/or the most helpful side task. For p-CNN, the loss weights and losses for the side tasks behave similarly to those of m-CNN. For the two main tasks, the dynamic-weighting scheme assigns a higher loss weight to the easier task at the moment. Their losses reduce in a similar way, i.e., the error reduction in one task will also contribute to the other.

Compare to other methods Table 1 shows that no prior work uses the entire Multi-PIE for face recognition. To compare with state of the art, we choose to use setting III to evaluate our method since it is the most challenging setting with all poses included. The network structures and parameter settings are exactly the same as those of the full set. As shown in Tab. 3, our s-CNN already outperforms c-CNN forest [36], which is an ensemble of three c-CNN models. This is attributed to the deep structure of CASIA-Net [38] compared to [36]. Moreover, our m-CNN and p-CNN further outperform s-CNN with significant margins, especially

	Avg.	$\pm 90^\circ$	$\pm 75^\circ$	$\pm 60^\circ$	$\pm 45^\circ$	$\pm 30^\circ$	$\pm 15^\circ$
FIP_20 [44]	67.87	34.13	47.32	61.64	78.89	89.23	95.88
FIP_40 [44]	70.90	31.37	49.10	69.75	85.54	92.98	96.30
c-CNN [36]	73.54	41.71	55.64	70.49	85.09	92.66	95.64
c-CNN Forest [36]	76.89	47.26	60.66	74.38	89.02	94.05	96.97
s-CNN (ours)	88.45	76.72	82.80	88.71	85.18	96.89	98.41
m-CNN (ours)	90.08	76.72	84.97	89.75	89.15	97.40	99.02
p-CNN (ours)	91.27	76.96	87.83	92.07	90.34	98.01	99.19

Table 3. Multi-PIE performance comparison in setting III of Tab. 1.

Method	Training Set	Metric	Acc(%)
DeepID2 [30]	P: 202, 599 / 10, 177	JB	95.43
DeepFace [32]	R: 4.4M / 4, 030	cos	95.92
CASIANet [38]	P: 494, 414 / 10, 575	cos	96.13
Wang et al. [34]	P: 404, 992 / 10, 553	JB	96.2
Littwin and Wolf [22]	P: 404, 992 / 10, 553	JB	98.14
MultiBatch [31]	R: 2.6M / 12K	Ed	98.20
VGG-DeepFace [26]	P: 2.6M / 2, 622	Ed	98.95
Wen et al. [35]	P: 0.7M / 17, 189	cos	99.28
FaceNet [28]	R: 260M / 8M	L2	99.63
s-CNN (ours)	P: 494, 414 / 10, 575	cos	97.87
m-CNN (ours)	P: 494, 414 / 10, 575	cos	98.07
p-CNN (ours)	P: 494, 414 / 10, 575	cos	98.27

Table 4. Performance comparison on LFW. Training set format: public (P) or private (R): total images / subjects. Metric includes Joint-Bayes (JB), cosine (cos), and Euclidean (Ed).

for non-frontal faces. We want to stress the improvement margin between our method 91.27% and the prior work of 76.89% — an relative error reduction of 62%. This huge margin is rarely seen in prior face recognition work, especially on a classic benchmark dataset, which is a testimony on our contribution to push the state of the art.

4.2. Unconstrained Face Recognition

Experimental settings We use CASIA-Webface [38] as our training set and evaluate on LFW [13], CFP [29], and IJB-A [19] datasets. CASIA-Webface consists of 494, 414 images of 10, 575 subjects. LFW consists of 10 folders each with 300 same-person pairs and 300 different-person pairs. Given the saturated performance of LFW mainly due to its mostly frontal view faces, CFP and IJB-A are introduced for large-pose face recognition. CFP is composed of 500 subjects each with 10 frontal and 4 profile images. Similar to LFW, CFP has 10 folders, each with 350 same-person pairs and 350 different-person pairs, for both frontal-frontal (FF) and frontal-profile (FP) experiments. IJB-A dataset includes 5, 396 images and 20, 412 video frames of 500 sub-

Method ↓	Frontal-Frontal			Frontal-Profile		
Metric (%) →	Accuracy	EER	AUC	Accuracy	EER	AUC
Sengupta et al. [29]	96.40 ± 0.69	3.48 ± 0.67	99.43 ± 0.31	84.91 ± 1.82	14.97 ± 1.98	93.00 ± 1.55
Sankarana. et al. [27]	96.93 ± 0.61	2.51 ± 0.81	99.68 ± 0.16	89.17 ± 2.35	8.85 ± 0.99	97.00 ± 0.53
Chen, et al. [6]	98.67 ± 0.36	1.40 ± 0.37	99.90 ± 0.09	91.97 ± 1.70	8.00 ± 1.68	97.70 ± 0.82
Human	96.24 ± 0.67	5.34 ± 1.79	98.19 ± 1.13	94.57 ± 1.10	5.02 ± 1.07	98.92 ± 0.46
s-CNN (ours)	97.34 ± 0.99	2.49 ± 0.09	99.69 ± 0.02	90.96 ± 1.31	8.79 ± 0.17	96.90 ± 0.08
m-CNN (ours)	97.77 ± 0.39	2.31 ± 0.06	99.69 ± 0.02	91.39 ± 1.28	8.80 ± 0.17	97.04 ± 0.08
p-CNN (ours)	97.79 ± 0.40	2.48 ± 0.07	99.71 ± 0.02	94.39 ± 1.17	5.94 ± 0.11	98.36 ± 0.05

Table 5. Performance comparison on CFP. Results reported are the average ± standard deviation over the 10 folds.

jects. It defines template-to-template matching for both face verification and identification.

In order to apply the proposed method, we need to have the labels for the side tasks. However, it is not easy to manually label our training set. Instead, we only consider pose estimation as the side task and use the estimated pose as the label. We use PIFA [17] to estimate 34 landmarks and the yaw angle, which defines three groups: right profile $[-90^\circ, -30^\circ]$, frontal $[-30^\circ, 30^\circ]$, and left profile $[30^\circ, 90^\circ]$. CASIA-Webface is biased towards frontal faces with 88% faces belonging to the frontal pose group based on our pose estimation. We modify our network structures slightly for CASIA-Webface dataset, with details provided in the supplementary material. We use the same pre-processing as in [38]. Each image is horizontally flipped for data augmentation. We also generate the mirror image of an input face in the testing stage. We use the average cosine distance of all four comparisons between the image pair and its mirror images for face comparison.

Performance on LFW Table 4 compares performance with state-of-the-art methods on LFW. We follow the unrestricted with labeled outside data protocol. We only compare CNN-based methods with a single model. Our implementation of the CASIA-Net (s-CNN) with BN achieves much better results compared to [38]. Even with such a high baseline, m-CNN and p-CNN can still improve, achieving comparable results with state of the art, or better results if comparing to the methods with the same amount of training data. Since LFW is biased towards frontal faces, we expect the improvement of our method to be larger if they are trained and tested on large-pose datasets.

Performance on CFP Table 5 shows the performance comparison with state-of-the-art methods on CFP. For FF experiments, m-CNN and p-CNN slightly improve the verification rate of s-CNN. This is expected, as there is little pose variation. For FP experiments, p-CNN substantially outperforms s-CNN and prior work in three evaluation metrics, reaching close-to-human performance. Note our accuracy of 94.39% is 30% relative error reduction of the previous state of the art 91.97%. Therefore, the proposed divide-and-conquer scheme is very effective in unconstrained face verification with large pose variation. Even with the estimated pose serving as the ground truth pose label for MTL,

Method ↓	Verification		Identification	
Metric (%) →	@FAR=1e-2	@FAR=1e-3	@Rank-1	@Rank-5
OpenBR [19]	23.6 ± 0.9	10.4 ± 1.4	24.6 ± 1.1	37.5 ± 0.8
GOTS [19]	40.6 ± 1.4	19.8 ± 0.8	44.3 ± 2.1	59.5 ± 2.0
Wang et al. [34]	72.9 ± 3.5	51.0 ± 6.1	82.2 ± 2.3	93.1 ± 1.4
PAM [23]	73.3 ± 1.8	55.2 ± 3.2	77.1 ± 1.6	88.7 ± 0.9
DCNN [5]	78.7 ± 4.3	–	85.2 ± 1.8	93.7 ± 1.0
s-CNN (ours)	75.6 ± 3.5	52.0 ± 7.0	84.3 ± 1.3	93.0 ± 0.9
m-CNN (ours)	75.6 ± 2.8	51.6 ± 4.5	84.7 ± 1.0	93.4 ± 0.7
p-CNN (ours)	77.4 ± 2.7	53.9 ± 4.3	85.8 ± 1.4	93.8 ± 0.9

Table 6. Performance comparison on IJB-A.

the models can still disentangle the pose variation from the learnt identity features for pose-invariant face verification.

Performance on IJB-A We conduct close-set face identification and face verification on IJB-A. First, we retrain our models after removing 26 overlapped subjects between CASIA-Webface and IJB-A. Second, we fine-tune the re-trained models on the IJB-A training set of each fold for 50 epoches. Similar to [34], we separate all images into “well-aligned” and “poorly-aligned” faces based on the face alignment results and the provided annotations. In the testing stage, we only select images from the “well-aligned” faces for recognition. If all images in a template are “poorly-aligned” faces, we select the best aligned face among them. Table 6 shows the performance comparison on IJB-A. Similarly, we only compare to the methods with a single model. The proposed p-CNN achieves comparable performance in face verification and identification. The margin between s-CNN and p-CNN shows the merit of MTL for unconstrained face recognition.

5. Conclusions

This paper explores multi-task learning for face recognition with PIE estimations as the side tasks. We propose a dynamic-weighting scheme to automatically assign the loss weights for each side task during training. MTL helps to learn more discriminative identity features by disentangling the PIE variations. We also propose a pose-directed multi-task CNN with stochastic routing scheme to direct different paths for face images with different poses. We make the first effort to study face identification on the entire Multi-PIE dataset with full PIE variations. Extensive experiments on Multi-PIE show that our m-CNN and p-CNN can dra-

matically improve face recognition performance, especially on large poses. The proposed method is applicable to in-the-wild datasets with estimated pose serving as the label for training. We have achieved state-of-the-art performance on LFW, CFP, and IJB-A, showing the value of MTL for pose-invariant face recognition in the wild.

References

- [1] A. H. Abdulnabi, G. Wang, J. Lu, and K. Jia. Multi-task CNN model for attribute prediction. *TMM*, 2015. 1
- [2] A. Argyriou, T. Evgeniou, and M. Pontil. Convex multi-task feature learning. *Machine Learning*, 2008. 2
- [3] A. Asthana, T. K. Marks, M. J. Jones, K. H. Tieu, and M. Rohith. Fully automatic pose-invariant face recognition via 3D pose normalization. In *ICCV*, 2011. 2
- [4] D. Chen, S. Ren, Y. Wei, X. Cao, and J. Sun. Joint cascade face detection and alignment. In *ECCV*, 2014. 1
- [5] J.-C. Chen, V. M. Patel, and R. Chellappa. Unconstrained face verification using deep cnn features. In *WACV*, 2016. 8
- [6] J.-C. Chen, J. Zheng, V. M. Patel, and R. Chellappa. Fisher vector encoded deep convolutional features for unconstrained face verification. In *ICIP*, 2016. 8
- [7] B. Chu, S. Romdhani, and L. Chen. 3D-aided face recognition robust to expression and pose variations. In *CVPR*, 2014. 3
- [8] C. Ding, C. Xu, and D. Tao. Multi-task pose-invariant face recognition. *IJP*, 2015. 2, 3
- [9] L. El Shafey, C. McCool, R. Wallace, and S. Marcel. A scalable formulation of probabilistic linear discriminant analysis: Applied to face recognition. *TPAMI*, 2013. 5
- [10] R. Gross, I. Matthews, J. Cohn, T. Kanade, and S. Baker. Multi-PIE. *IVC*, 2010. 2
- [11] H. Han, S. Shan, X. Chen, S. Lao, and W. Gao. Separability oriented preprocessing for illumination-insensitive face recognition. In *ECCV*, 2012. 3
- [12] H. Han, S. Shan, L. Qing, X. Chen, and W. Gao. Lighting aware preprocessing for face recognition across varying illumination. In *ECCV*, 2010. 3
- [13] G. B. Huang, M. Ramesh, T. Berg, and E. Learned-Miller. Labeled faces in the wild: A database for studying face recognition in unconstrained environments. Technical report, Technical Report 07-49, University of Massachusetts, Amherst, 2007. 2, 7
- [14] S. Ioffe and C. Szegedy. Batch normalization: Accelerating deep network training by reducing internal covariate shift. *arXiv preprint:1502.03167*, 2015. 3
- [15] S. Ji and J. Ye. An accelerated gradient method for trace norm minimization. In *ICML*, 2009. 2
- [16] Y. Jia, E. Shelhamer, J. Donahue, S. Karayev, J. Long, R. Girshick, S. Guadarrama, and T. Darrell. Caffe: Convolutional architecture for fast feature embedding. In *ACMMM*, 2014. 5
- [17] A. Jourabloo and X. Liu. Large-pose face alignment via CNN-based dense 3D model fitting. In *CVPR*, 2016. 8
- [18] M. Kan, S. Shan, H. Chang, and X. Chen. Stacked progressive auto-encoders (SPAe) for face recognition across poses. In *CVPR*, 2014. 3
- [19] B. F. Klare, B. Klein, E. Taborsky, A. Blanton, J. Cheney, K. Allen, P. Grother, A. Mah, M. Burge, and A. K. Jain. Pushing the frontiers of unconstrained face detection and recognition: IARPA Janus Benchmark A. In *CVPR*, 2015. 2, 7, 8
- [20] S. Li, X. Liu, X. Chai, H. Zhang, S. Lao, and S. Shan. Morphable displacement field based image matching for face recognition across pose. In *ECCV*, 2012. 2, 3
- [21] Y. Li, B. Zhang, S. Shan, X. Chen, and W. Gao. Bagging based efficient kernel fisher discriminant analysis for face recognition. In *ICPR*, 2006. 4
- [22] E. Littwin and L. Wolf. The multiverse loss for robust transfer learning. In *CVPR*, 2016. 1, 7
- [23] I. Masi, S. Rawls, G. Medioni, and P. Natarajan. Pose-aware face recognition in the wild. In *CVPR*, 2016. 2, 8
- [24] I. Misra, A. Shrivastava, A. Gupta, and M. Hebert. Cross-stitch networks for multi-task learning. In *CVPR*, 2016. 2
- [25] V. Nair and G. E. Hinton. Rectified linear units improve restricted boltzmann machines. In *ICML*, 2010. 3
- [26] O. M. Parkhi, A. Vedaldi, and A. Zisserman. Deep face recognition. In *BMVC*, 2015. 7
- [27] S. Sankaranarayanan, A. Alavi, C. Castillo, and R. Chellappa. Triplet probabilistic embedding for face verification and clustering. *arXiv preprint:1604.05417*, 2016. 8
- [28] F. Schroff, D. Kalenichenko, and J. Philbin. Facenet: A unified embedding for face recognition and clustering. In *CVPR*, 2015. 1, 7
- [29] S. Sengupta, J.-C. Chen, C. Castillo, V. M. Patel, R. Chellappa, and D. W. Jacobs. Frontal to profile face verification in the wild. In *WACV*, 2016. 2, 7, 8
- [30] Y. Sun, Y. Chen, X. Wang, and X. Tang. Deep learning face representation by joint identification-verification. In *NIPS*, 2014. 1, 7
- [31] O. Tadmor, Y. Wexler, T. Rosenwein, S. Shalev-Shwartz, and A. Shashua. Learning a metric embedding for face recognition using the minibatch method. In *NIPS*, 2016. 7
- [32] Y. Taigman, M. Yang, M. Ranzato, and L. Wolf. Deepface: Closing the gap to human-level performance in face verification. In *CVPR*, 2014. 1, 7
- [33] Y. Tian, P. Luo, X. Wang, and X. Tang. Pedestrian detection aided by deep learning semantic tasks. In *CVPR*, 2015. 1, 2, 4
- [34] D. Wang, C. Otto, and A. K. Jain. Face search at scale. *TPAMI*, 2016. 7, 8
- [35] Y. Wen, K. Zhang, Z. Li, and Y. Qiao. A discriminative feature learning approach for deep face recognition. In *ECCV*, 2016. 1, 5, 7
- [36] C. Xiong, X. Zhao, D. Tang, K. Jayashree, S. Yan, and T.-K. Kim. Conditional convolutional neural network for modality-aware face recognition. In *ICCV*, 2015. 2, 3, 4, 7
- [37] M. Yang, L. Gool, and L. Zhang. Sparse variation dictionary learning for face recognition with a single training sample per person. In *ICCV*, 2013. 3
- [38] D. Yi, Z. Lei, S. Liao, and S. Z. Li. Learning face representation from scratch. *arXiv preprint:1411.7923*, 2014. 3, 7, 8

- [39] J. Yim, H. Jung, B. Yoo, C. Choi, D. Park, and J. Kim. Rotating your face using multi-task deep neural network. In *CVPR*, 2015. [1](#), [2](#), [4](#)
- [40] C. Zhang and Z. Zhang. Improving multiview face detection with multi-task deep convolutional neural networks. In *WACV*, 2014. [1](#), [2](#)
- [41] H. Zhang, Y. Zhang, and T. S. Huang. Pose-robust face recognition via sparse representation. *Pattern Recognition*, 2013. [3](#), [4](#)
- [42] Z. Zhang, P. Luo, C. C. Loy, and X. Tang. Facial landmark detection by deep multi-task learning. In *ECCV*, 2014. [1](#)
- [43] X. Zhu, Z. Lei, J. Yan, D. Yi, and S. Z. Li. High-fidelity pose and expression normalization for face recognition in the wild. In *CVPR*, 2015. [3](#)
- [44] Z. Zhu, P. Luo, X. Wang, and X. Tang. Deep learning identity-preserving face space. In *ICCV*, 2013. [2](#), [7](#)
- [45] Z. Zhu, P. Luo, X. Wang, and X. Tang. Multi-view perceptron: A deep model for learning face identity and view representations. In *NIPS*, 2014. [2](#), [3](#), [4](#)